ACS APPLIED MATERIALS & INTERFACES

Letter

www.acsami.org

Size Selective Photoetching of CdSe Quantum Dot Sensitizers on Single-Crystal TiO_2

Justin B. Sambur*,† and Bruce A. Parkinson‡

†Department of Chemistry and Chemical Biology, Cornell University, Ithaca, New York 14853, United States

‡Department of Chemistry and School of Energy Resources, University of Wyoming, Laramie, Wyoming 82071, United States

ABSTRACT: Cadmium selenide quantum dots covalently attached to and photosensitizing single-crystal TiO_2 surfaces are observed to corrode under illumination in aqueous electrolyte containing iodide as a regenerator. Comparison of photocurrent spectra before and after long-term monochromatic illumination indicated that the CdSe QD sensitizers photocorroded and decreased in size until their band gap energy exceeded the excitation energy. This wavelength-dependent photoelectrochemical etching mechanism can be used to tune the size distribution of surface adsorbed QDs and may account for the instability of QD sensitized solar cells that do not employ sulfide-based electrolytes.

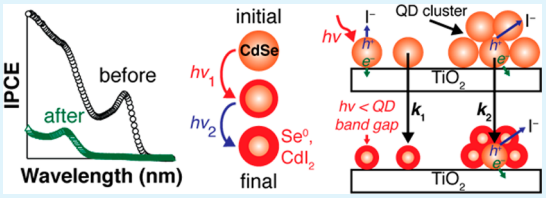

KEYWORDS: *quantum dots (QDs), quantum dot sensitized solar cells (QDSSCs), single-crystal TiO_2, stability, corrosion, size-selective etching*

It has been proposed that semiconductor nanocrystals or quantum dots (QDs) may be superior sensitizers to molecular dyes because they potentially offer increased visible-light absorption, enhanced stability due to their inorganic nature, low-temperature solution processing, and the possibility to exceed the Shockley–Queisser limit.[1−3] However, the power conversion efficiency of QD sensitized solar cells (QDSSCs) is not yet competitive with that of dye sensitized solar cells (DSSCs). One strategy to improve the power conversion efficiency of QDSSCs is to tune the redox potential of the electrolyte in order to increase the open circuit potential of the device.[4] However, for metal chalcogenide QD sensitizers, the electrolyte composition has a significant impact on long-term chemical stability under illumination.[5] For example, it is often observed that the most efficient I^-/I_3^- redox electrolyte employed for DSSCs leads to a rapid photocurrent decay when employed in metal chalcogenide QDSSCs.[6] This observation is consistent with the well-established anodic corrosion process observed for bulk metal chalcogenide electrodes that occurs in the absence of a chemically stabilizing redox electrolyte, such as a basic solution containing S^{2-}/S_n^{2-}.[7−9] Studies that exclusively focus on the stability of devices are rarely reported and details of the photochemical degradation process have not been elucidated.

Alternatively, photocorrosion of colloidal semiconductor nanoparticles has been studied in great detail. Henglein first demonstrated photoetching of small CdS particles under band gap illumination in aqueous solution.[10] Later studies demonstrated that, by varying the excitation wavelength, the average particle size of a semiconductor colloid suspension could be precisely tuned by photochemical etching.[11,12] Photochemical etching exploits the acute relationship between particle size and optical band gap of small semiconductor particles.[13] So-called "size-selective" photoetching has been demonstrated using a variety of colloidal semiconductor nanoparticles including CdS,[11,12,14] CdSe,[15,16] CdTe,[17,18] InP,[19] PbS,[20] ZnS,[12] ZnTe,[17] and ZnO.[12] The mechanism of particle decomposition seemed to follow the same anodic corrosion process observed for bulk electrode materials.[11,12] For example, Memming and co-workers identified Cd^{2+} and SO_4^{2-} as corrosion products of photoelectrochemically etched *n*-type CdS single-crystal electrodes in aqueous electrolyte[21] and Matsumoto et al. observed the production of SO_4^{2-} during the photocorrosion of CdS nanocrystals in aerated aqueous solutions.[11]

Although photocorrosion has an undesirable effect for energy conversion applications, the technique can be used to prepare near monodisperse particle distributions for the study of quantum size effects. Photochemical size-selective etching has the potential to decrease the average particle size as much as 30 Å and narrow the size distribution by 30%.[12] Furthermore, Khon et al. demonstrated that photochemical etching could be used to selectively etch domains of a multicomponent CdSe/CdS nanorod/nanoparticle dimer to improve the photocalaytic activity.[22] In this letter, we report a size-selective etching mechanism to describe the photodegradation process of CdSe QD sensitizers in aerated aqueous iodide electrolytes.

MPA-capped CdSe QDs (MPA-CdSe QDs) adsorbed on bulk single crystal TiO_2 substrates were investigated as model QDSSCs. The (100) face of an undoped rutile single crystal and the (001) face of a naturally occurring anatase crystal (doping density = 10^{18} cm^{-3} by Mott–Schottky analysis) were sensitized from the same solution of purified MPA-CdSe QDs

Received: November 13, 2014
Accepted: December 5, 2014
Published: December 5, 2014

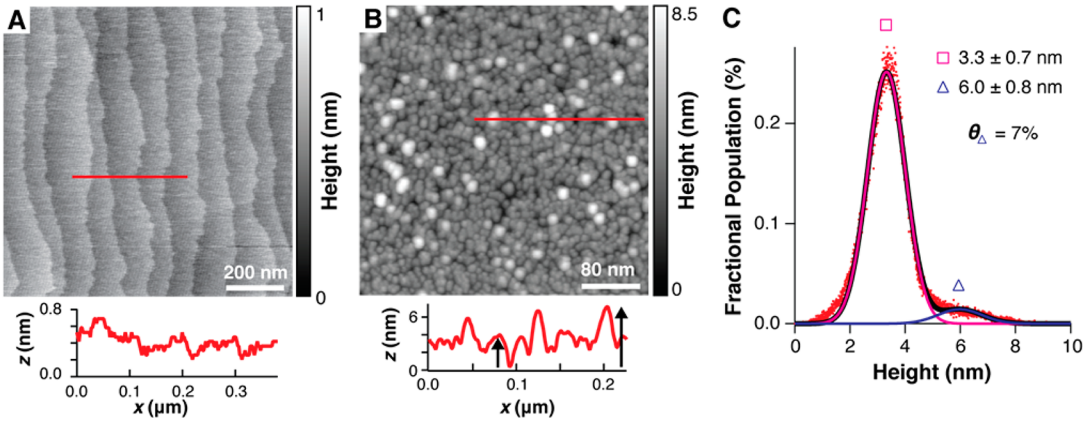

Figure 1. AFM images of the (A) bare rutile (100) substrate and (B) MPA-capped CdSe QDs adsorbed on the same substrate. The height profiles below each image were measured from the solid red line in A and B. (C) Red dots indicate the histogram of the distribution of heights from all pixels in B, plotted as a fractional population where the sum of all bins is 100%. The solid pink and blue lines represent Gaussian fits to the data (red dots). The pink square and blue triangle represents the average height from each Gaussian fit. The solid black line represents the sum of the two Gaussian fits. The relative surface coverage of QD clusters $\theta_{clusters}$ was determined by comparing the relative contribution of the 6.0 nm height population (minor fractional component) to the 3.3 nm height population (see main text for details).

according to previously published procedures.[23,24] Atomic force microscopy (AFM) was used to characterize the QD surface coverage and morphology (e.g., single layer or multilayer QDs) of the undoped rutile substrate and the anatase crystal was mounted as a working electrode for photoelectrochemical measurements according to previously published procedures.[23] Figure 1A shows a tapping mode AFM image of the bare rutile (100) TiO_2 surface. The height profile (bottom Figure 1A) of the substrate exhibited 50−100 nm wide terraces that are nearly atomically flat. The AFM image in Figure 1B shows the same rutile (100) surface covered with MPA-CdSe QDs. The height profile (bottom Figure 1B) measured across low and high contrast features of the QD-coated substrate indicated two height transitions (indicated by black arrows in the height profile). To quantitatively determine the height and relative populations of QDs that contribute to the two height transitions, we analyzed the distribution of heights of every pixel of Figure 1B. Figure 1C shows the histogram of the distribution of height data from every pixel (red dots). Two distinct height populations were observed, consistent with the line profile data in Figure 1B. We fit the major and minor fractional populations with Gaussian functions and determined average heights of 3.3 ± 0.7 nm and 6.0 ± 0.8 nm, respectively. The average 3.3 ± 0.7 nm height of the major population agrees well with the expected 3.8 nm QD diameter inferred from optical absorbance data of the sample.[25] We therefore attribute the major fractional population to a single layer of CdSe QDs. Since the minor population was nearly double in height to the single layer of QDs, we attribute this surface feature to QD clusters that are two QDs high. Due to tip effects and the high surface coverage of QDs, it is difficult to quantify the cluster diameter from x−y measurements. Nonetheless, we determined the relative surface coverage of QD clusters by integrating the individual Gaussians and dividing the total QD cluster coverage from the total single layer QD coverage to yield the relative surface coverage of QD clusters ($\theta_{clusters}$ = 7% for the image in Figure 1B). We repeated this procedure for 5 different AFM images and determined an average $\theta_{clusters}$ = 6 ± 2%. In summary, the sensitization procedure results in a >90% single-layer QD coverage with some clusters consisting of two QDs in height.

Independent measurements of unmounted anatase crystals showed that the surface coverage of QDs was similar to that of Figure 1B and did not strongly depend on the specific crystal face or polymorph of TiO_2.[23] Using the mounted anatase (001) electrode, we initially studied the stability of the sensitized photocurrent under constant monochromatic illumination in an aerated 0.25 M KI electrolyte. Figure 2A shows the incident

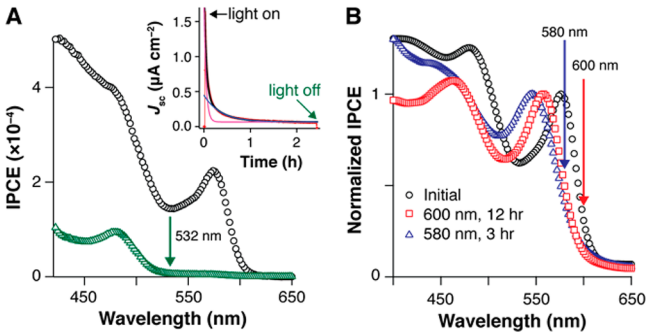

Figure 2. (A) IPCE spectra of MPA-capped CdSe QDs adsorbed on an anatase (001) electrode surface measured before (black circles) and after (green triangles) 20 h of 47.7 mW cm^{-2} illumination at 532 nm in an aqueous iodide (0.25 M KI) electrolyte at short circuit versus a Pt wire. The inset shows the short circuit photocurrent versus time data (red dots) for the first 2 h of illumination. The solid black line represents a double exponential fit to the data (see main text) and the individual components are represented as pink and blue lines. (B) IPCE spectra normalized to the values at the maxima of the excitonic features measured on the anatase (001) electrode before (black circles) and after 12 h of continuous 30 μW cm^{-2} 600 nm illumination (red squares) and after an additional 3 h of continuous 30 μW cm^{-2} 580 nm illumination (blue triangles).

photon to current efficiency (IPCE) spectra of the CdSe QD sensitized electrode before (black circles) and after (green triangles) 20 h of continuous 532 nm laser illumination (47.7 mW cm^{-2}). The initial photocurrent spectrum exhibited a first exciton peak at 574 nm that closely matched the peak position observed in the optical absorbance spectrum of the colloidal QD sample (average diameter equal to 3.8 nm).[24] After long-term illumination at 532 nm, the IPCE values decreased

dx.doi.org/10.1021/am507974h | ACS Appl. Mater. Interfaces 2014, 6, 21916−21920

significantly over the entire wavelength range. Specifically, only 2 and 4% of the initial IPCE value remained at the first exciton peak (574 nm) and the incident illumination wavelength (532 nm), respectively. In addition, a 94 nm blue shift in the first exciton peak was observed in the photocurrent spectrum after long-term illumination. The exciton peak shift to higher photon energy indicated an increase in the QD band gap that could be attributed to a 1.8 nm decrease in particle diameter.[25] Moreover, the onset of photocurrent occurred at approximately 530 nm, coinciding with the incident photon energy used during long-term illumination.

We fit the first exciton peaks in Figure 2A with Gaussian functions and determined that the full width at half-maximum increased by 45% after long-term illumination; the same trend can be observed in Figure 2B. The increased peak width after photoetching indicated that the heterogeneity in particle size distribution had increased. This trend is opposite to reports of narrowing size distributions from photochemical etching of noninteracting QDs in colloidal suspensions[12] and may be due to varying degrees of surface passivation of surface adsorbed QDs, either from QD-QD or QD-TiO_2 interactions, that leads to a wide distribution of particle sizes after photoetching.

To further understand the decay process, we analyzed the sensitized photocurrent decay versus illumination time for the first 2.4 h of 532 nm laser illumination (inset Figure 2A). We observed that the sensitized photocurrent at 532 nm after 2.4 h illumination was 4% of the initial photocurrent (J_0) and was equal to the ratio of IPCE values at 532 nm after 20 h illumination (4%, as discussed previously). Thus, under these experimental conditions, the sensitized photocurrent decayed rapidly to a small, stable photocurrent equal to $0.04J_0$. Thus, we fit the photocurrent−time data with a double exponential function with a constant photocurrent offset, $A_1 \exp(-(x/\tau_1)) + A_2 \exp(-(x/\tau_2)) + y_0$, to yield $A_1 = 1736 \pm 2$ μA cm^{-2}, $\tau_1 = 2.68 \pm 0.01$ min, $A_2 = 383 \pm 1$ μA cm^{-2}, $\tau_2 = 21.71 \pm 0.07$ min, and $y_0 = 65.8 \pm 0.1$ μA cm^{-2} ($R^2 = 0.998$, error bars are 95% confidence intervals). The fit parameters indicated that the majority of the photocurrent decays in approximately 3 min and a minor component of the photocurrent signal decays on an approximately 10× longer time scale.

Photocurrent spectroscopy was used to further elucidate the photoelectrochemical corrosion mechanism of CdSe QD sensitizers on TiO_2 in aqueous iodide electrolytes. Figure 2B shows the normalized IPCE spectra of CdSe QDs before and after monochromatic illumination at different photon energies. The exciton peak at 576 nm, corresponding to the initial core CdSe QD photocurrent spectrum (black circles), was not altered after prolonged exposure to the aqueous iodide electrolyte in the dark. After 12 h of 600 nm illumination (30 μW cm^{-2}), the exciton peak is blue-shifted to 558 nm (red circles). After further illumination of the same electrode with 580 nm wavelength photons (blue triangles), the exciton peak is further shifted to shorter wavelengths (546 nm). Thus, photocurrent spectroscopy revealed a decrease in the CdSe QD particle size upon illumination with photon energies larger than the nanocrystal band gap. The photoelectrochemical corrosion process ceased when the incident photon energy was less than the nanocrystal band gap, thus defining the size of the nanocrystal. It is notable that we and others have previously observed that CdSe QDs sensitizers are stable under band gap illumination for extended periods (>30 h) in sulfide/polysulfide electrolytes.[6,23]

This size-selective etching phenomenon was previously observed in colloidal QD samples and the mechanism agreed with earlier work using bulk polycrystalline or single crystal electrodes. For bulk CdSe photoanodes, early work by Gerisher,[7] Hodes,[9] and Wrighton[8] established that the photocorrosion products in aqueous electrolyte were soluble Cd^{2+} ions and a surface layer of Se. Elemental Se has been identified as a corrosion product in CdSe QDSSCs.[5] Although we did not identify the potentially small amount of corrosion products leached from or deposited onto the surfaces of the CdSe QD sensitizers, we propose a photocorrosion mechanism (described in eqs 1-3) based on these previous studies to explain the degradation of CdSe QD sensitizers operating in iodide electrolytes. Equation 1 represents the formation of electron−hole pairs in CdSe QDs upon supra band gap monochromatic illumination. The exciton is separated at the TiO_2/QD/electrolyte interface via electron injection into the TiO_2 conduction band and hole transfer to the I^- acceptor (eq 2). However, the sensitized system is not chemically stable to reduction by I^- and thus anodic oxidation of CdSe from photoexcited holes causes dissolution of Cd and deposition of elemental Se or CdI_2 on the nanocrystal surface (eq 3).

$$\mathrm{CdSe} + h\nu \rightarrow \mathrm{CdSe}(e^- + h^+) \quad (1)$$

$$\mathrm{CdSe}(e^- + h^+) + \mathrm{TiO_2} + \mathrm{I^-} \rightarrow \mathrm{I^{3-}} + \mathrm{TiO_2}(e^-) \quad (2)$$

$$\mathrm{CdSe} + 2h^+ \rightarrow \mathrm{Cd^{2+}} + \mathrm{Se^0} \quad (3)$$

We further propose that the QD surface morphology affects the photoelectrochemical etching rate according to Scheme 1.

Scheme 1. Proposed Morphology-Dependent Size-Selective Photoetching Mechanism of CdSe QDs on Single-Crystal TiO_2

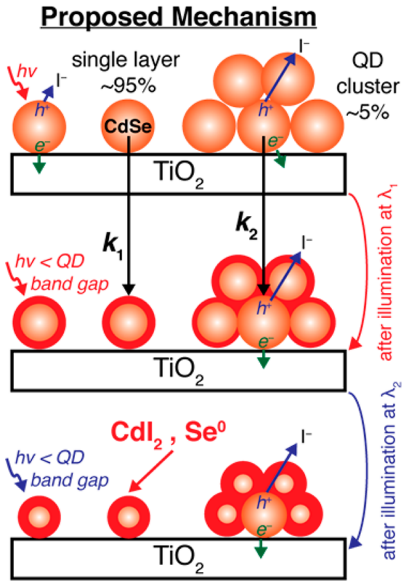

The top row of Scheme 1 shows a cartoon illustration of the CdSe QD/TiO_2 interface whereby ~95% of the surface consists of a single layer of QDs and ~5% of the surface consists of QD clusters (based on analysis described in Figure 1C). Upon exposure to monochromatic illumination, the QDs inject electrons into the TiO_2 electrode. The sensitized photocurrent decays until the majority of QDs decrease in size until their band gap exceeds the excitation energy (middle row, Scheme

1). We observed that 4% of the initial photocurrent is retained at the excitation wavelength after long-term illumination (inset Figure 2A). Since the sensitized photocurrent is proportional to the QD surface coverage, we propose that the ∼5% residual sensitized photocurrent at the excitation wavelength can be attributed QD clusters whose surface coverage is ∼5%. The QDs underneath clusters may be partially passivated by surrounding QDs of the cluster and remain intact, which accounts for the small, persistent photocurrent at long illumination times (middle and bottom rows of Scheme 1). Based on the relative amplitudes of A_1 and A_2 obtained from fitting the photocurrent−time data, we assign the smaller amplitude component A_2 to the QD clusters. Thus, the majority of single layer QDs etch at a rate k_1 and partially passivated QDs within clusters etch at a slower rate k_2, where $k_1 \approx 10 \times k_2$. In this scenario, the pathway of charge carriers from QDs beneath clusters involves electron injection into TiO_2 and the holes are transported across a neighboring QD and through a CdI_2 or Se corrosion layer. This transport mechanism is plausible because (i) holes can be transported through multiple QDs[26] and (ii) we observed sensitized photocurrent from corroded QDs when higher energy photons are used; hole transport across the corrosion layer is possible.

In summary, we report an excitation wavelength-dependent, size-selective photoelectrochemical etching process for CdSe QDs covalently attached to TiO_2 electrodes. We propose that the CdSe core decreases in size due to photoanodic corrosion, resulting in deposition of elemental Se or CdI_2 on the nanocrystal surface. The etching process ceases when the nanocrystal decreases in size and its light absorption threshold is higher in energy than the incident illumination. If the sample is further excited by supra band gap illumination, the etching process continues and the QDs further decrease in size. Quantitative comparison of the QD surface coverage and the residual sensitized photocurrent at the excitation wavelength suggested that the QD surface morphology affects the photoetching rate. We propose that partially passivated QDs beneath clusters etch ∼10× slower than the majority of single layer QDs. The results have potential implications for the stability of QDSSC devices and QD solar cells where the possibility of QD stacking interactions is increased by the three-dimensional architecture QDs on the TiO_2 electrode.

AUTHOR INFORMATION

Corresponding Author

*E-mail: jbs427@cornell.edu.

Notes

The authors declare no competing financial interest.

ACKNOWLEDGMENTS

The authors wish to acknowledge the U.S. Department of Energy, Office of Science, Basic Energy Sciences, Division of Chemical Sciences, Geosciences and Biosciences for financial support through grant DE-FG03-96ER14625.

REFERENCES

(1) Hodes, G. Comparison of Dye- and Semiconductor-Sensitized Porous Nanocrystalline Liquid Junction Solar Cells. *J. Phys. Chem. C* **2008**, *112*, 17778−17787.

(2) Kamat, P. V. Quantum Dot Solar Cells. Semiconductor Nanocrystals as Light Harvesters. *J. Phys. Chem. C* **2008**, *112*, 18737−18753.

(3) Sambur, J. B.; Novet, T.; Parkinson, B. A. Multiple Exciton Collection in a Sensitized Photovoltaic System. *Science* **2010**, *330*, 63−66.

(4) Jun, H. K.; Careem, M. A.; Arof, A. K. Quantum Dot-Sensitized Solar Cells—Perspective and Recent Developments: A Review of Cd chalcogenide Quantum Dots as Sensitizers. *Renewable Sustainable Energy Rev.* **2013**, *22*, 148−167.

(5) Wang, K.; He, W.; Wu, L.; Xu, G.; Ji, S.; Ye, C. On the Stability of CdSe Quantum Dot-Sensitized Solar Cells. *RSC Adv.* **2014**, *4*, 15702−15708.

(6) Lee, Y.-L.; Chang, C.-H. Efficient Polysulfide Electrolyte for CdS Quantum Dot-Sensitized Solar Cells. *J. Power Sources* **2008**, *185*, 584−588.

(7) Gerischer, H.; Mindt, W. The Mechanisms of the Decomposition of Semiconductors by Electrochemical Oxidation and Reduction. *Electrochim. Acta* **1968**, *13*, 1329−1341.

(8) Ellis, A. B.; Kaiser, S. W.; Bolts, J. M.; Wrighton, M. S. Study of *n*-Type Semiconducting Cadmium Chalcogenide-Based Photoelectrochemical Cells Employing Polychalcogenide Electrolytes. *J. Am. Chem. Soc.* **1977**, *99*, 2839−2848.

(9) Hodes, G.; Manassen, J.; Cahen, D. Photoelectrochemical Energy Conversion and Storage Using Polycrystalline Chalcogenide Electrodes. *Nature* **1976**, *261*, 403−404.

(10) Henglein, A. Photo-Degradation and Fluorescence of Colloidal-Cadmium Sulfide in Aqueous Solution. *Ber. Bunsen. Phys. Chem.* **1982**, *86*, 301−305.

(11) Matsumoto, H.; Sakata, T.; Mori, H.; Yoneyama, H. Preparation of Monodisperse CdS Nanocrystals by Size Selective Photocorrosion. *J. Phys. Chem.* **1996**, *100*, 13781−13785.

(12) van Dijken, A.; Janssen, A. H.; Smitsmans, M. H. P.; Vanmaekelbergh, D.; Meijerink, A. Size-Selective Photoetching of Nanocrystalline Semiconductor Particles. *Chem. Mater.* **1998**, *10*, 3513−3522.

(13) Brus, L. E. A Simple Model for the Ionization Potential, Electron Affinity, and Aqueous Redox Potentials of Small Semiconductor Crystallites. *J. Chem. Phys.* **1983**, *79*, 5566−5571.

(14) Matsumoto, H.; Sakata, T.; Mori, H.; Yoneyama, H. Narrowing Size Distribution of CdS Nanocrystals by Size Selective Photocorrosion. *Chem. Lett.* **1995**, *24*, 595−596.

(15) Torimoto, T.; Murakami, S.-y.; Sakuraoka, M.; Iwasaki, K.; Okazaki, K.-i.; Shibayama, T.; Ohtani, B. Photochemical Fine-Tuning of Luminescent Color of Cadmium Selenide Nanoparticles: Fabricating a Single-Source Multicolor Luminophore. *J. Phys. Chem. B* **2006**, *110*, 13314−13318.

(16) Galian, R. E.; de la Guardia, M.; Pérez-Prieto, J. Photochemical Size Reduction of CdSe and CdSe/ZnS Semiconductor Nanoparticles Assisted by nπ* Aromatic Ketones. *J. Am. Chem. Soc.* **2009**, *131*, 892−893.

(17) Resch, U.; Weller, H.; Henglein, A. Photochemistry and Radiation Chemistry of Colloidal Semiconductors. 33. Chemical Changes and Fluorescence in CdTe and ZnTe. *Langmuir* **1989**, *5*, 1015−1020.

(18) Uematsu, T.; Kitajima, H.; Kohma, T.; Torimoto, T.; Tachibana, Y.; Kuwabata, S. Tuning of the Fluorescence Wavelength of CdTe quantum dots with 2 nm Resolution by Size-Selective Photoetching. *Nanotechnology* **2009**, *20*, 215302.

(19) Talapin, D. V.; Gaponik, N.; Borchert, H.; Rogach, A. L.; Haase, M.; Weller, H. Etching of Colloidal InP Nanocrystals with Fluorides: Photochemical Nature of the Process Resulting in High Photoluminescence Efficiency. *J. Phys. Chem. B* **2002**, *106*, 12659−12663.

(20) Liu, J.; Aruguete, D. M.; Jinschek, J. R.; Donald Rimstidt, J.; Hochella, M. F., Jr The Non-Oxidative Dissolution of Galena Nanocrystals: Insights Into Mineral Dissolution Rates as a Function of Grain Size, Shape, and Aggregation State. *Geochim. Cosmochim. Acta* **2008**, *72*, 5984−5996.

(21) Meissner, D.; Memming, R.; Kastening, B. Photoelectrochemistry of Cadmium Sulfide. 1. Reanalysis of Photocorrosion and Flat-Band Potential. *J. Phys. Chem.* **1988**, *92*, 3476−3483.

(22) Khon, E.; Lambright, K.; Khnayzer, R. S.; Moroz, P.; Perera, D.; Butaeva, E.; Lambright, S.; Castellano, F. N.; Zamkov, M. Improving the Catalytic Activity of Semiconductor Nanocrystals through Selective Domain Etching. *Nano Lett.* **2013**, *13*, 2016−2023.
(23) Sambur, J. B.; Riha, S. C.; Choi, D.; Parkinson, B. A. Influence of Surface Chemistry on the Binding and Electronic Coupling of CdSe Quantum Dots to Single Crystal TiO_2 Surfaces. *Langmuir* **2010**, *26*, 4839−4847.
(24) Sambur, J. B.; Parkinson, B. A. CdSe/ZnS Core/Shell Quantum Dot Sensitization of Low Index TiO_2 Single Crystal Surfaces. *J. Am. Chem. Soc.* **2010**, *132*, 2130−2131.
(25) Yu, W. W.; Qu, L.; Guo, W.; Peng, X. Experimental Determination of the Extinction Coefficient of CdTe, CdSe, and CdS Nanocrystals. *Chem. Mater.* **2003**, *15*, 2854−2860.
(26) Kern, M. E.; Watson, D. F. Linker-Assisted Attachment of CdSe Quantum Dots to TiO_2: Time- and Concentration-Dependent Adsorption, Agglomeration, and Sensitized Photocurrent. *Langmuir* **2014**, *30*, 13293−13300.